



Plasma-photocatalytic conversion of CO₂ at low temperatures: Understanding the synergistic effect of plasma-catalysis



Danhua Mei^a, Xinbo Zhu^a, Chunfei Wu^{b,c}, Bryony Ashford^a, Paul T. Williams^b, Xin Tu^{a,*}

^a Department of Electrical Engineering and Electronics, University of Liverpool, Liverpool L69 3GJ, UK

^b School of Chemical & Process Engineering, University of Leeds, Leeds LS2 9JT, UK

^c School of Engineering, University of Hull, Hull HU6 7RX, UK

ARTICLE INFO

Article history:

Received 23 June 2015

Received in revised form

23 September 2015

Accepted 28 September 2015

Keywords:

Plasma-catalysis

Dielectric barrier discharge

CO₂ conversion

Synergistic effect

Energy efficiency

ABSTRACT

A coaxial dielectric barrier discharge (DBD) reactor has been developed for plasma-catalytic conversion of pure CO₂ into CO and O₂ at low temperatures (<150 °C) and atmospheric pressure. The effect of specific energy density (SED) on the performance of the plasma process has been investigated. In the absence of a catalyst in the plasma, the maximum conversion of CO₂ reaches 21.7% at a SED of 80 kJ/L. The combination of plasma with BaTiO₃ and TiO₂ photocatalysts in the CO₂ DBD slightly increases the gas temperature of the plasma by 6–11 °C compared to the CO₂ discharge in the absence of a catalyst at a SED of 28 kJ/L. The synergistic effect from the combination of plasma with photocatalysts (BaTiO₃ and TiO₂) at low temperatures contributes to a significant enhancement of both CO₂ conversion and energy efficiency by up to 250%. The UV intensity generated by the CO₂ discharge is significantly lower than that emitted from UV lamps that are used to activate photocatalysts in conventional photocatalytic reactions, which suggests that the UV emissions generated by the CO₂ DBD only play a very minor role in the activation of the BaTiO₃ and TiO₂ catalysts in the plasma-photocatalytic conversion of CO₂. The synergy of plasma-catalysis for CO₂ conversion can be mainly attributed to the physical effect induced by the presence of catalyst pellets in the discharge and the dominant photocatalytic surface reaction driven by the plasma.

© 2015 Elsevier B.V. All rights reserved.

1. Introduction

Recently, the abatement of carbon dioxide (CO₂) has become a major global challenge as CO₂ is the main greenhouse gas and its emissions lead to the problems of climate change and global warming. Different strategies are being developed to tackle the challenges associated with CO₂ emissions, including carbon capture and storage (CCS), carbon capture and utilization (CCU), reducing fossil fuel consumption and boosting clean and renewable energy use. Direct conversion of CO₂ into value-added fuels and chemicals (e.g. CO, CH₄, and methanol) offers an attractive route for efficient utilization of low value CO₂ whilst significantly reducing CO₂ emissions [1]. However, CO₂ is a highly stable and non-combustible molecule, requiring considerable energy for upgrading and activation. Various synthetic approaches for CO₂ conversion have been explored, including solar driven photochemical reduction [2], electrochemical reduction [3] and thermal catalysis [4]. Despite their potential, further investigation into the development

of cost-effective H₂ production methods, novel multifunctional catalysts and new catalytic processes are essential to improve the overall energy efficiency of CO₂ conversion processes and the product selectivity to practical and implementable levels.

Non-thermal plasma technology provides a promising alternative to the traditional catalytic route for the conversion of CO₂ into value-added fuels and chemicals at ambient conditions [5]. In non-thermal plasmas, highly energetic electrons and chemically reactive species (e.g. free radicals, excited atoms, ions, and molecules) can be generated for the initiation of both physical and chemical reactions. Non-thermal plasma has a distinct non-equilibrium character, which means the gas temperature in the plasma can be close to room temperature, whilst the electrons are highly energetic with a typical mean energy of 1–10 eV [6]. As a result, non-thermal plasma can easily break most chemical bonds (e.g. C–O bonds), and enable thermodynamically unfavourable chemical reactions (e.g. CO₂ decomposition) to occur at ambient conditions. However, the use of plasma alone leads to low selectivity and yield towards the target end-products, and consequently causes low energy efficiency of the plasma processes. Recently, the combination of plasma with catalysis, known as plasma-catalysis, has attracted tremendous interest for environmental clean-up,

* Corresponding author.

E-mail addresses: xin.tu@liverpool.ac.uk, tuxinzj2000@gmail.com (X. Tu).

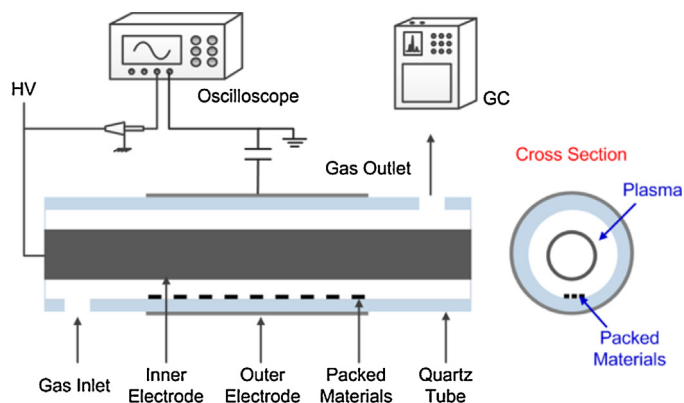


Fig. 1. Schematic diagram of the experimental setup.

greenhouse gas reforming, growth of carbon nanomaterials, ammonia synthesis and catalyst treatment [6–13]. The integration of plasma and solid catalysts has great potential to generate a synergistic effect, which can activate the catalysts at low temperatures and improve their activity and stability, resulting in the remarkable enhancement of reactant conversion, selectivity and yield of target products, as well as the energy efficiency of the plasma process [6]. Direct conversion of CO₂ into valuable CO and O₂ has been explored using different non-thermal plasmas [5,14–25]. However, most previous works have mainly focused on the conversion of CO₂ diluted with noble gases (e.g. He and Ar), which is not preferable from an industrial application point of view [14,22,25]. Further fundamental work is still required to optimize and improve the energy efficiency of the plasma process. In addition, finding a suitable and cost-effective catalyst for this reaction to enhance the overall efficiency of the process is a great challenge as very limited work has been focused on plasma-catalytic CO₂ conversion. A detailed understanding of the synergistic effect resulting from the combination of plasma and photocatalysts at low temperatures is still required due to gaps in current knowledge resulting in only a vague idea of the interactions occurring. For example, it is not clear what the roles are of UV light and highly energetic electrons generated by the plasma in the plasma-photocatalytic chemical reactions.

In this work, a coaxial dielectric barrier discharge (DBD) has been developed for the plasma-photocatalytic conversion of pure CO₂ into CO and O₂ at low temperatures. The effect of photocatalysts (BaTiO₃ and TiO₂) on the temperatures (plasma gas temperature and the temperature on the catalyst surface) in the CO₂ DBD has been evaluated. The synergistic effect resulting from the combination of plasma and photocatalysts (BaTiO₃ and TiO₂) for CO₂ conversion has been investigated from both

without dilution at a flow rate of 15–60 mL/min. The DBD reactor was supplied by an AC high voltage power supply with a peak-to-peak voltage of 10 kV and a frequency of 50 Hz. All the electrical signals were sampled by a 4-channel digital oscilloscope (TDS2014). Different catalyst pellets BaTiO₃ (TCU) and TiO₂ (Alfa Aesar) with a diameter of 1 mm were packed into the discharge gap along the bottom of the quartz tube. Our previous work demonstrated that this packing method induces effective plasma-catalyst interactions, which might generate a synergistic effect and hence promote plasma-catalytic chemical reactions [6]. The gas temperature and the temperature on the surface of the catalysts in the DBD reactor were measured by a fiber optical temperature probe (Omega, FOB102), which was placed in the plasma area. X-ray diffraction (XRD) patterns of the fresh catalyst samples were recorded by a Siemens D5000 diffractometer using Cu-K α radiation in the 2θ range between 10° and 70°. X-ray photoelectron spectroscopic (XPS) measurements were carried out on a PerkinElmer PHI-5400 XPS system with mono-chromatic Mg K α (1253.6 eV) X-rays with a data acquisition system. The spectra are referenced to C1s peak at 284.5 eV. The UV intensity generated by the CO₂ DBD with and without a catalyst was measured by an UV meter (Omega HHUVA1). The gas products were analyzed by a two-channel gas chromatography (Shimadzu 1014) equipped with a flame ionization detector (FID) and a thermal conductivity detector (TCD). The concentration of ozone was measured by an ozone monitor (2B, Model 106-M). To evaluate the performance of the plasma process, the specific energy density (SED), CO₂ conversion (C_{CO_2}), selectivity towards CO and O₂ (S_{CO} and S_{O_2}), carbon and oxygen balance (B_{Carbon} and B_{Oxygen}) as well as energy efficiency (E) are defined as follows:

$$SED \text{ (kJ/L)} = \frac{\text{Discharge power (kW)}}{\text{CO}_2 \text{ flow rate (L/s)}} \quad (1)$$

$$C_{CO_2} \text{ (%) } = \frac{\text{CO}_2 \text{ converted (mol/s)}}{\text{CO}_2 \text{ input (mol/s)}} \times 100 \quad (2)$$

$$S_{CO} \text{ (%) } = \frac{\text{CO produced (mol/s)}}{\text{CO}_2 \text{ converted (mol/s)}} \times 100 \quad (3)$$

$$S_{O_2} \text{ (%) } = \frac{\text{O}_2 \text{ produced (mol/s)}}{\text{CO}_2 \text{ converted (mol/s)}} \times 100 \quad (4)$$

$$B_{Carbon} \text{ (%) } = \frac{\text{CO}_2 \text{ unconverted (mol/s)} + \text{CO produced (mol/s)}}{\text{CO}_2 \text{ input (mol/s)}} \times 100 \quad (5)$$

$$B_{Oxygen} \text{ (%) } = \frac{2 \times \text{CO}_2 \text{ unconverted (mol/s)} + \text{CO produced (mol/s)} + 2 \times \text{O}_2 \text{ produced (mol/s)}}{2 \times \text{CO}_2 \text{ input (mol/s)}} \times 100 \quad (6)$$

physical and chemical perspectives for the first time.

2. Experimental

In this study, a coaxial DBD reactor has been developed for the plasma-catalytic reduction of pure CO₂ into CO and O₂ at atmospheric pressure and low temperatures (<150 °C), as shown in Fig. 1. An Al foil (ground electrode) was wrapped around the outside of a quartz tube with an external diameter of 22 mm and an inner diameter of 19 mm. A stainless steel tube with an outer diameter of 14 mm was used as the inner electrode (high voltage electrode). The discharge gap was fixed at 2.5 mm, whilst the discharge length was varied from 90 to 150 mm. CO₂ was used as the feed gas

$$E \text{ (mmol/kJ)} = \frac{\text{CO}_2 \text{ converted (mmol/s)}}{\text{Discharge power (kW)}} \quad (7)$$

3. Results and discussion

3.1. Plasma-assisted conversion of CO₂ without catalyst

Fig. 2 shows the effect of SED on the conversion of CO₂ and the energy efficiency of the plasma reaction in the absence of a catalyst. Clearly, increasing the specific energy density significantly enhances CO₂ conversion due to the increase in energy input to the discharge. The conversion of CO₂ is increased by a factor of 3 (from 6.7 to 21.7%) as the SED rises from 8 to 80 kJ/L. Similar conversion trends have been reported either using plasma alone or

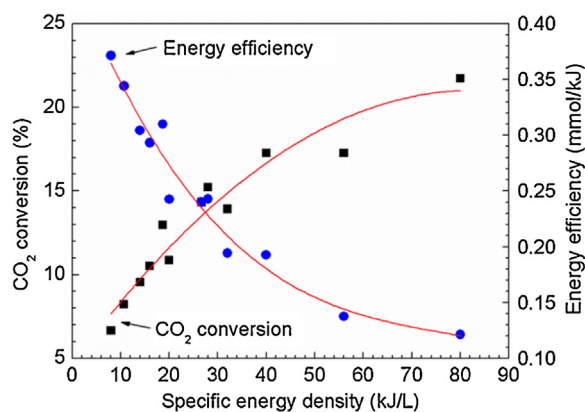


Fig. 2. CO₂ conversion and energy efficiency as a function of SED.

using plasma-catalysis for chemical reactions [26,27]. Our previous works have shown that increasing energy input by changing applied voltage at a constant frequency could effectively increase the number of microdischarges and enhance the density of energetic electrons, as well as the gas temperature in the discharge [28–30], all of which may contribute in different ways to the improvement in conversion. Moreover, increasing the discharge power produces more chemically reactive species (e.g. O atoms), which can further induce CO₂ dissociation to enhance its conversion. A lower feed gas flow rate was reported to be beneficial for improving the conversion of reactants due to longer retention time of the reactants in the plasma. In contrast, the specific energy density has an opposite effect on the energy efficiency of the plasma process. Increasing the SED from 8 to 80 kJ/L leads to a decrease of the energy efficiency from 0.37 to 0.12 mmol/kJ, which is consistent with previous results [31]. In this work, the maximum energy efficiency of 0.37 mmol/kJ is achieved at the lowest specific energy density of 8 kJ/L with a discharge power of 8 W, a CO₂ feed flow rate of 60 mL/min and a discharge length of 150 mm.

CO₂ dissociation by electron impact vibrational excitation (Eqs. (8) and (9)) is believed to be the most effective pathway for CO₂ conversion in non-thermal plasmas, which can lead to a high energy efficiency of more than 60% [32].



where ν^* is the vibrational excited state. Up to 97% of the total plasma energy can be transferred from electrons to vibrational excitation of CO₂ if the plasma discharges have an electron temperature of 1–2 eV, or a reduced electric field (E/N) of 20–40 Td [32]. Recent plasma modeling of CO₂ splitting in a DBD reactor showed that in a CO₂ discharge with an average electron energy of 2–3 eV, only 12% of the energy can be allocated to vibrational states, whereas ~79% goes to electronic excited states, and ~4% and ~5% can be transferred to dissociation and ionization of CO₂, respectively [33]. Their results showed that the majority (94%) of CO₂ conversion is induced by reactions (e.g. dissociation) with ground state CO₂ (shown in Eq. (10)) and only 6% of CO₂ conversion occurs through reactions with vibrational excited CO₂ at a high electric field [33].



In this study, the average electric field E in the CO₂ DBD without a catalyst is estimated to be around 1.75 kV/mm under our experimental conditions, obtained from Lissajous figure [10], while the corresponding mean electron energy of the plasma is around 2.4 eV, calculated using BOLSIG+ code based on electron energy distribution function (EEDF) [34]. This result suggests that the

electron impact dissociation of CO₂ might play a dominant role in CO₂ conversion in this experiment.

The electron impact dissociation of CO₂ in its vibrational excited states (Eq. (9)) or ground state (Eq. (10)) will most likely result in CO in its ground state ($^1\Sigma$) and O atoms in both the ground state (3P) and metastable state (1D). However, since CO bands were observed in the emission spectra of the CO₂ discharge generated in a similar coaxial DBD reactor, CO could also be formed in excited states [6].

Oxygen can be formed from the 3-body recombination of atomic oxygen (Eq. (11)) or from the reaction with a ground state CO₂ molecule (Eq. (12)).



Oxygen might also be generated directly by electron impact dissociation of CO₂ if the electron has a high energy (>15 eV).



In this study, no carbon deposition is observed after the plasma conversion of CO₂ with and without catalyst. The main gas products from plasma conversion of pure CO₂ were CO and O₂. The selectivities towards CO and O₂ are in the range of 91.5–96.7% and 45.4–48.5%, respectively, while the carbon balance (98.1–99.5%) and oxygen balance (98.0–99.6%) are very high. This agrees with recent experimental and modeling works in which CO and O₂ were identified as the main products in the conversion of CO₂ when using DBD [33,35]. Ozone could be formed by the following reaction:



However, ozone was not detected in this work. Ozone could be decomposed by local heating generated by the plasma in the reactor. Semiokhin and Andrev suggested that oxygen formed from CO₂ dissociation could be initially converted into O₃, followed by ozone decomposition into O₂ through electron impact reactions [36]. In contrast, recent plasma modeling of CO₂ conversion showed that the calculated fractional density of O₃ was only 0.05% in a similar DBD reactor [33]. In addition, the maximum rate for ozone formation in the DBD reactor was two orders of magnitude lower than that of the three-body recombination of atomic oxygen for O₂ production [33]. It is worth noting that gas heating was not calculated explicitly in the model, which might be able to explain the difference in ozone formation in the experiment and modeling. Our previous study has shown the formation of CO and CO₂⁺ spectra in a similar DBD containing CO₂ using optical emission spectroscopic diagnostics [6], which suggests that electron impact ionization of CO₂ occurs in the plasma CO₂ reaction.



The recorded CO₂⁺ spectra also reveal the formation of highly energetic electrons in the CO₂ discharge as the electron impact ionization of CO₂ requires electrons with a high energy of at least 13.8 eV.

3.2. Plasma-photocatalytic conversion of CO₂

The effect of BaTiO₃ and TiO₂ photocatalysts on the conversion of CO₂ is shown in Fig. 3. It is clear that the presence of both BaTiO₃ and TiO₂ in the discharge significantly enhances the CO₂ conversion and energy efficiency of the plasma process. Packing BaTiO₃ pellets into the discharge gap exhibits exceptional performance with a remarkable enhancement of both CO₂ conversion (from 15.2 to 38.3%) and energy efficiency (from 0.24 to 0.60 mmol/kJ) by a factor of 2.5 at a SED of 28 kJ/L.

The plasma gas temperature and the temperature on the catalyst surface in the plasma conversion of CO₂ have been measured in the

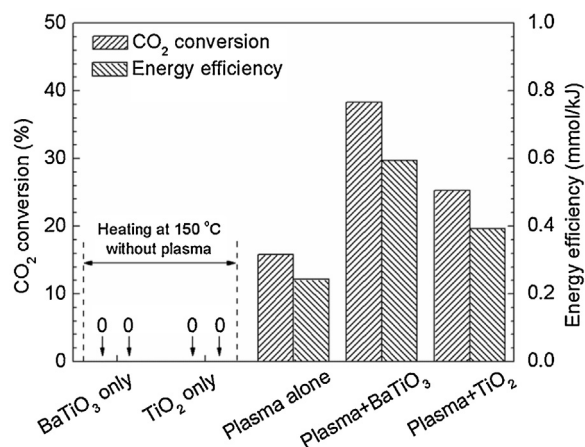


Fig. 3. Demonstration of the synergistic effect of plasma-catalysis for the conversion of CO₂ (SED = 28 kJ/L).

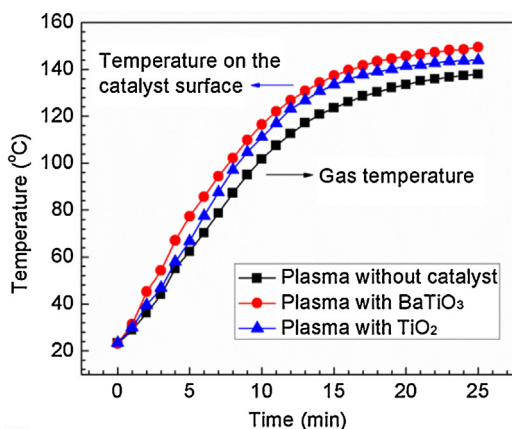


Fig. 4. Plasma gas temperature and the temperature on the surface of BaTiO₃ and TiO₂ catalysts in the CO₂ DBD reactor (SED = 28 kJ/L). Note that the gas temperature of the CO₂ DBD and the temperature on the catalyst surface are almost the same when the catalyst (BaTiO₃ and TiO₂) is placed in the plasma zone.

DBD reactor at a SED of 28 kJ/L, as shown in Fig. 4. Clearly, the plasma gas temperature of the CO₂ DBD without a catalyst significantly increases from 23.3 to 123.5 °C in the first 15 min after igniting the plasma, after which it rises slowly and is almost constant (~138 °C) at 25 min when the plasma reaches a stable state. Similar evolution behaviour of the temperature can also be observed in the plasma-catalysis system (Fig. 4). In the CO₂ DBD reactor partially packed with the BaTiO₃ and TiO₂ catalysts, we note that the plasma temperature in the gas phase and the temperature on the catalyst surface are almost the same. Thus, only one temperature (the temperature on the catalyst surface) is shown in Fig. 4 to present the temperature in the plasma-catalysis system. It is interesting to note that the combination of plasma with the BaTiO₃ and TiO₂ catalysts slightly increases the gas temperature (TiO₂: ~144 °C and BaTiO₃: ~149 °C) of the CO₂ discharge by 6–11 °C compared to the CO₂ DBD in the absence of a catalyst at the same SED of 28 kJ/L. This phenomenon might be attributed to inelastic electron-molecule collisions in the plasma-catalytic processes [12,37,38].

To understand the role of plasma in the reaction, a purely thermal experiment has been carried out by heating both photocatalysts in a pure CO₂ flow at 150 °C. No conversion and adsorption of CO₂ was observed. Thermodynamic equilibrium calculation of the CO₂ reaction has also confirmed that the conversion of CO₂ is almost zero at low temperatures (e.g. 150 °C), suggesting that an extremely low CO₂ conversion is expected from the thermal catalytic

reduction of CO₂ when carried out at the same temperature as that used in the plasma reaction (see Fig. S11 in the Supporting information). The results clearly show that the exceptional reaction performance has been achieved by the use of plasma-catalysis, which is much higher than the sum of plasma-alone and catalysis alone, indicating the formation of a synergistic effect when combining plasma with photocatalysts at low temperatures.

Catalysts can be integrated into a DBD system in different ways. The presence of the catalyst pellets in part of the gas gap still shows predominantly filamentary discharges and surface discharges on the catalyst surface, which induces effective interactions between plasma and catalyst for CO₂ activation. In this work, the dielectric constant of BaTiO₃ and TiO₂ is 10,000 and 85, respectively. Previous experimental [39,40] and simulation [41,42] studies have shown that packing catalyst pellets, especially pellets with a high dielectric constant (e.g. BaTiO₃), into the discharge gap can generate a non-uniform electric field with enhanced electric field strength near contact points between the pellets and the pellet-dielectric wall. The maximum local electric field near these contact points can be much higher than that in the void in a plasma-catalysis reactor, depending on the contact angle, curvature and dielectric constant of the materials [43]. The space (including the space filled with pellets) averaged electric field in a plasma fully packed with packing pellets is initially increased by a factor of 1.4 when increasing the dielectric constant of the materials from 10 to 1000, above this the change in the electric field becomes negligible [43]. We have reported that the interaction of plasma and TiO₂ exhibited a strong effect on the electron energy distribution in the discharge with an increase in both highly energetic electrons and electric field [29]. This phenomenon can also be confirmed by previous work, showing that the presence of TiO₂ in a plasma leads to a significant increase of the reduced electric field [44]. These results suggest that the presence of the catalyst pellets in the plasma gap play a crucial role in inducing physical effects, such as enhancement of the electric field and production of more energetic electrons and reactive species, which in turn leads to chemical effects and contributes to the conversion of CO₂. In this study, the average electric field is increased by 10.9% and 9.0% with the presence of BaTiO₃ and TiO₂ in the discharge gap, respectively; whilst the corresponding mean electron energy is increased by 11.3% and 9.4% (see Fig. S12 in the Supporting information). Both of these effects contribute to the enhancement of the CO₂ conversion.

However, the enhancement of the reaction performance in terms of CO₂ conversion and energy efficiency is found to be more significant than only due to the changes in plasma physical parameters (e.g. average electric field). This suggests that in addition to the plasma physical effect and the resulting gas phase reactions (Eqs. (8)–(15)), the contribution of a plasma-activated photocatalytic reaction to the synergy of plasma-catalysis cannot be ruled out. The XRD patterns of the samples show that BaTiO₃ has the tetragonal phase, while TiO₂ exhibits the crystal structure of anatase (see Fig. S13 in the Supporting information). TiO₂ is a widely used photocatalyst with a wide band gap of 3.2 eV for anatase phase, while BaTiO₃ is a perovskite semiconductor photocatalyst with a band gap of 2.8–3.0 eV for tetragonal phase. It is well known that photocatalysts can be activated through the formation of electron-hole (e[−]–h⁺) pairs with the aid of sufficient photonic energy ($h\nu$) with an appropriate wavelength to overcome the band-gap between the valence band and the conductive band [45]:



Plasma discharges can generate UV radiation without using any extra UV sources (e.g. UV lamps). This has been confirmed by the dominated N₂ (C-B) bands (between 300 nm and 400 nm) in a CO₂

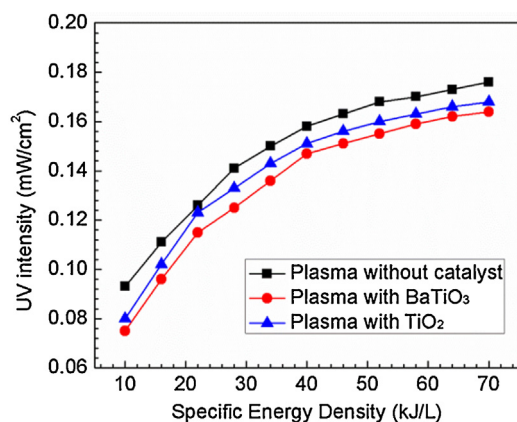


Fig. 5. UV intensity generated by the CO₂ DBD with and without a catalyst as a function of SED.

DBD in our previous work [6,46]. However, UV radiation generated by plasma discharges is not always the controlling factor to activate photocatalysts due to its low intensity compared to that emitted by an UV lamp [47]. In this work, we have measured the UV intensity generated by the CO₂ DBD with and without a catalyst, as shown in Fig. 5. In the absence of a catalyst in the DBD reactor, the UV intensity produced by the CO₂ discharge is about 0.141 mW/cm² at a SED of 28 kJ/L. When the BaTiO₃ and TiO₂ photocatalysts are placed in the plasma zone, the UV intensity of the CO₂ discharge is decreased to 0.115 mW/cm² and 0.123 mW/cm², respectively. Note that these values are significantly lower than the UV intensity (~20–60 mW/cm²) produced from UV lamps to activate photocatalysts in conventional photocatalytic reactions [48–50], which suggests that the UV emissions generated by the CO₂ discharge only play a minor role in the activation of the BaTiO₃ and TiO₂ photocatalysts. Similar results have been reported in the previous papers [51,52]. Assadi et al. found that the UV light generated by a surface DBD was too weak to activate TiO₂ photocatalyst for the removal of 3-methylbutanal (3MBA) [51]. Sano et al. reported that the UV intensity emitted by a N₂/O₂ surface discharge was only 2.5 μW/cm² at an input power of 5 W. The contribution of the plasma UV activated photocatalytic reaction to the overall performance of acetaldehyde decomposition was less than 0.2% [52].

Whitehead has suggested that electron-hole pairs can be created by electron impact upon the surface of photocatalysts since DBD can generate electrons of very similar energy (3–4 eV) to the photons [13,53], as shown in Eqs. (18) and (19). Nakamura et al. have also reported that photocatalysts can be activated by plasma and the electrons can be trapped onto the formed oxygen vacancies (V_o) to enhance the photoexcitation process [54].

In this work, the exceptional performance of the plasma-catalytic CO₂ conversion has been achieved through the combination of plasma and photocatalysts. However, the significant enhancement of the reaction performance in terms of CO₂ conversion and energy efficiency cannot only be attributed to the changes in plasma physical parameters (e.g. increased average electric field), as the estimated average electric field and mean electron energy in the CO₂ DBD are only increased by around 10% when the BaTiO₃ and TiO₂ catalysts are placed in the plasma zone. Furthermore, we find that the UV radiation generated by the CO₂ DBD is significantly weak compared to that produced from UV lamps, which suggests that it might only play a minor role in the photocatalytic activation of CO₂, and its contribution to the exceptional performance of the plasma-catalytic reaction and the synergy of plasma-photocatalysis could be very weak or negligible. In this study, the highly energetic electrons generated by plasma are

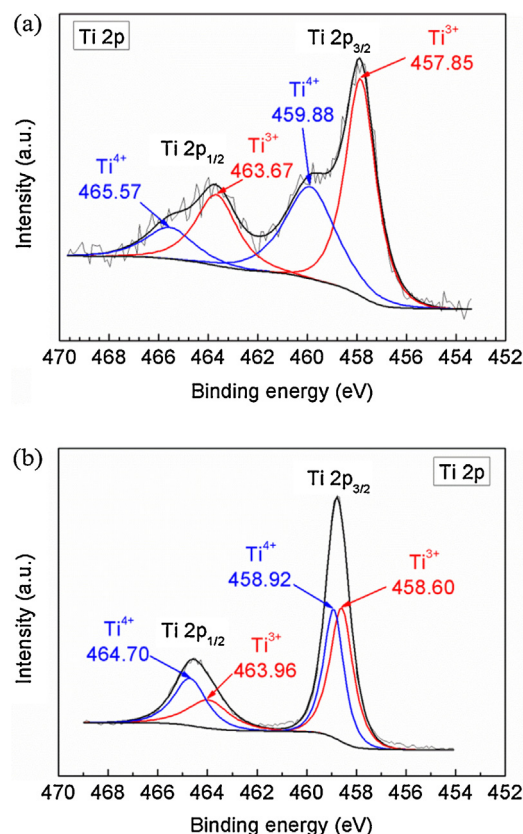
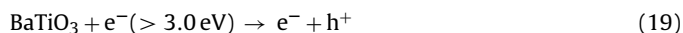


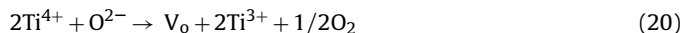
Fig. 6. XPS spectra of Ti 2p peaks for (a) BaTiO₃; and (b) TiO₂.

considered as the main driving force to activate the photocatalysts for CO₂ conversion.



Previous investigation has shown that the photocatalytic conversion of CO₂ is a multistep process, which involves the adsorption and subsequent activation of CO₂ molecules on the surface of photocatalysts and the subsequent dissociation of the C–O bond. The key step is the activation of CO₂ molecules through the transfer of trapped electrons to adsorbed CO₂ molecules in the V_o [55].

However, the recombination rate of electron-hole pairs is 2–3 orders of magnitude faster than that of charge separation and transfer in a defect-free photocatalyst, which will limit the efficiency of CO₂ conversion [55]. The defect disorders in photocatalysts, such as V_o, play an important role in the CO₂ reduction processes. V_o has been considered as the active site for the adsorption and activation of reactants in a photocatalytic reaction [56]. In this study, XPS measurement has been performed to investigate the surface structure and element valence of the photocatalysts. Fig. 6a shows the deconvolution spectra of Ti 2p in the BaTiO₃ sample. Two components (Ti 2p_{3/2} and Ti 2p_{1/2}) are identified and can be deconvoluted into 4 peaks. Two peaks at higher binding energy (459.88 and 465.57 eV) are assigned to the formal valence of Ti (4+) in BaTiO₃; whilst the Ti 2p_{3/2} and Ti 2p_{1/2} peaks of Ti³⁺ are located at around 457.85 eV and 463.67 eV. The presence of Ti³⁺ in the BaTiO₃ sample demonstrates the formation of V_o on the catalyst surface through the following reaction [57,58]:



where O²⁻ is the lattice oxygen. Clearly, the formation of V_o is followed by the change in the oxidative state of the vicinal Ti from Ti⁴⁺

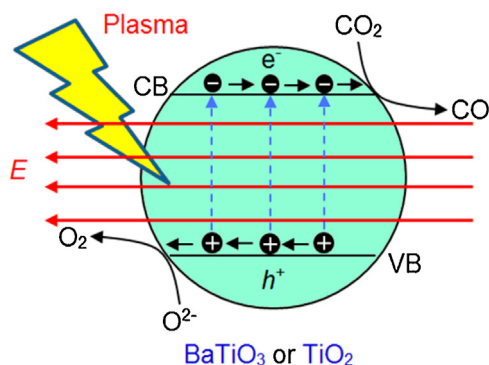
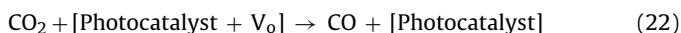


Fig. 7. Reaction mechanisms of plasma-photocatalytic conversion of CO₂ on the surface of photocatalysts.

to Ti³⁺ to retain the balance of local charge. Similarly, the Ti 2p_{3/2} and Ti 2p_{1/2} peaks of Ti³⁺ can also be detected in the XPS profile of TiO₂, as shown in Fig. 6b. We find that there are more Ti³⁺ species in the BaTiO₃ (60.9%) sample than in the TiO₂ (49.9%), which suggests more active sites (V_o) were formed in the BaTiO₃ catalyst, resulting in the higher CO₂ conversion using the BaTiO₃ catalyst.

Moreover, the combination rate of electron–hole pairs can also be significantly reduced in a plasma-photocatalytic system due to the presence of the electric field and the interactions between the plasma and photocatalyst [59]. In this study, the process of plasma-photocatalytic conversion of CO₂ can be described by Fig. 7. The electron (e[−])–hole (h⁺) pairs are generated with the aid of highly energetic electrons from the gas discharge, and are moved in the opposite direction by the electric field, which can reduce the probability of recombination. In the electron transfer process, CO₂ adsorbed in the V_o is reduced to the anion radical CO₂^{•−} by electrons from e[−]–h⁺ pairs (Eq. (21)), followed by the decomposition of CO₂^{•−} into CO and the occupation of one oxygen atom in the V_o site. The overall reaction is expressed in Eq. (22) [55,60], in which [Photocatalyst + V_o] and [Photocatalyst] represent the defective and defect-free photocatalysts, respectively.



In addition, V_o can be regenerated by oxidizing the surface O^{2−} anions using holes, followed by releasing O₂, as shown in Eq. (23). To balance the charge, the Ti⁴⁺ in the vicinity of the regenerated V_o can be reduced to Ti³⁺ by electrons [55,61,62], as shown in Eq. (24). This cyclic healed-regeneration of the oxygen vacancies maintains the equilibrium of the active sites in the photocatalysts and controls the conversion of CO₂, which can be confirmed by our experimental results as the CO₂ conversion did not change significantly when the plasma discharge was on for nearly two hours.

Therefore, we find that the synergistic effect resulting from the integration of DBD and photocatalysis for CO₂ conversion at low temperatures (without extra heating) can be attributed to the physical effect induced by the presence of photocatalysts in the discharge and the dominant photocatalytic surface reaction driven by the discharge.

3.3. Energy efficiency

Fig. 8 shows a comparison of the energy efficiency for CO₂ conversion using different atmospheric pressure non-thermal plasmas. It is clear that the energy efficiency (0.60 mmol/kJ) of the plasma

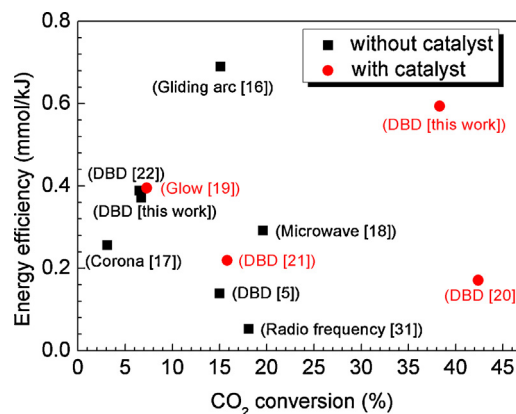


Fig. 8. Comparison of energy efficiency for CO₂ conversion with different atmospheric pressure plasma processes.

CO₂ conversion in the presence of photocatalysts (BaTiO₃) in this work is much higher than most of the other plasma processes regardless of the catalyst used. As shown in Fig. 8, the maximum energy efficiency of 0.69 mmol/kJ was achieved when the pure CO₂ decomposition was performed in an AC gliding arc discharge at a feed flow rate of 1.31 L/min. However, the corresponding conversion of CO₂ in this process was only 15.1%, which is significantly lower than that (38.3%) obtained in this work. A balance between CO₂ conversion and energy efficiency in the plasma processing of CO₂ is significantly important for the development and deployment of an efficient and cost-effective plasma process for CO₂ conversion and utilization [17]. In this work, the combination of DBD and photocatalysts (BaTiO₃ and TiO₂) leads to a significant enhancement in the CO₂ conversion and energy efficiency of the plasma process, as well as a balance between them. It is also interesting to note that the energy efficiency obtained in this work (DBD) is much higher than that of similar chemical reactions using a conventional packed bed DBD reactor where materials and/or catalysts are fully packed into the discharge gap [63]. In our previous works, we found that packing catalysts into the entire discharge zone led to a strong packed-bed effect and was found to shift the discharge mode from a typical strong filamentary microdischarge across the gap to a combination of surface discharge and weak microdischarge due to a significant reduction in the discharge volume [6,10,64]. As a result, only limited surface discharge can be generated on part of the catalyst surface and spatially limited microdischarges generated in the void space between pellet–pellet and pellet–quartz wall [10,40]. The formation of strong filamentary discharges in a DBD reactor without a catalyst is strongly suppressed when the solid catalysts are fully packed into the discharge gap. It is well known that a packed-bed effect can enhance the electric field in the plasma, which contributes to the enhancement of the reaction performance to some extent. However, such a significant transition in behaviour of the discharge mode induced by the strong packed bed effect (fully packed) could substantially reduce the performance of plasma-catalytic conversion or reforming processes for energy and fuel production, as catalysts placed in the plasma area might not be fully interacted and activated by the spatially limited discharges and weak interactions between the plasma and catalyst [6,10]. Our previous work has clearly shown that how to pack catalysts in a DBD reactor is of primary importance to induce strong physical and chemical interactions between the plasma and catalyst, which consequently affects the generation of the synergistic effect of the plasma-catalytic reaction, especially for the conversion of undiluted reactants to valuable fuels and chemicals [6].

One may argue that as packed-bed DBD reactors have been demonstrated to be effective at removing a wide range of low

concentration (10–1000 ppm) environmental gas pollutants [43], they could also be beneficial in the conversion of undiluted reactants. However, the major reaction mechanisms involved in the removal of dilute and low concentration gas pollutants and in the conversion of undiluted reactants (e.g. CO₂ or a mixture of CO₂ and CH₄) are significantly different due to different concentrations of reactants in the plasma chemical reactions. In the former reactions, highly energetic electrons mainly collide with carrier gas (e.g. air) to generate chemically reactive species (e.g. O, O₃, OH and N₂ (A)), which play dominant roles in the stepwise decomposition and oxidation of low concentration (ppm level) pollutants into CO, CO₂, H₂O and other by-products [65]. In contrast, electron impact reactions with reactants (e.g. CO₂) make significant contributions to the conversion of undiluted reactants in the latter reactions as carrier gases (e.g. N₂ and Ar) are not preferable. The transition behaviour of the discharge mode resulting in weak interactions of plasma and catalyst induced by the packed bed effect might not be so important in the former reactions since the increased electric field in the packed bed DBD reactor might be sufficient to produce reactive species for the removal of pollutants of ppm level. In addition, even a catalyst support (e.g. γ -Al₂O₃ and SiO₂) placed in a packed bed DBD reactor could absorb or decompose some gas pollutants of low concentration [66,67], leading us to think that the negative effect caused by the weak interaction between the plasma and packing catalysts (or supports) might be insignificant in the removal of dilute gas pollutants.

Further improvement in the energy efficiency of this process can be expected from the optimization of the plasma power and the design of new catalysts (e.g. coating metal nanoparticles on the photocatalysts). For example, previous simulation work has suggested that the energy efficiency of a plasma reactor can be enhanced by a factor of 4 when using rectangular pulses instead of a sinusoidal voltage [68].

The high reaction rate and fast attainment of steady state in plasma processes allow rapid start-up and shutdown of the process compared to thermal treatment, whilst plasma systems can also work efficiently with a rather small and compact size. This offers flexibility for plasma-catalytic processes to be integrated with renewable energy sources such as waste energy from wind power, as the surplus energy could provide cheap waste electricity for powering the plasma-catalytic process, making it more effective in reducing CO₂ emissions.

4. Conclusions

In this study, plasma-photocatalytic conversion of CO₂ into CO and O₂ has been investigated using a DBD reactor combined with BaTiO₃ and TiO₂ photocatalysts. The combination of plasma with the BaTiO₃ and TiO₂ photocatalysts in the CO₂ DBD slightly increases the gas temperature of the plasma by 6–11 °C compared to the CO₂ discharge in the absence of a catalyst at a SED of 28 kJ/L, while the plasma gas temperature in the gas phase is almost the same as the temperature on the surface of the photocatalysts (BaTiO₃ and TiO₂) in the plasma-catalytic DBD reactor. The combination of plasma with BaTiO₃ and TiO₂ catalysts has shown a synergistic effect, which significantly enhances the conversion of CO₂ and the energy efficiency by a factor of 2.5 compared to the plasma reaction in the absence of a catalyst. The presence of the catalyst pellets in the plasma gap is found to play a dominant role in inducing plasma physical effects, such as the enhancement of the electric field and production of more energetic electrons and reactive species, which in turn leads to chemical effects and partly contributes to the conversion of CO₂. We find that the intensity of UV emissions generated in the CO₂ DBD is significantly lower than that emitted from external UV sources (e.g. UV lamps)

that are commonly used to activate photocatalysts in conventional photocatalytic reactions. This phenomenon suggests that the UV emissions generated by the CO₂ DBD only play a minor role in the activation of the BaTiO₃ and TiO₂ catalysts in the plasma-photocatalytic conversion of CO₂, and its contribution to the achieved exceptional performance of the plasma-photocatalytic reaction and the synergy of plasma-photocatalysis could be very weak or negligible. In this study, the highly energetic electrons generated by plasma have been considered as the main driving force to activate the photocatalysts for CO₂ conversion. The overall synergistic effect resulting from the integration of DBD with photocatalysis for CO₂ conversion at low temperatures (without extra heating) can be attributed to both the physical effect induced by the presence of the catalyst in the discharge and the dominant photocatalytic surface reaction driven by energetic electrons from the CO₂ discharge.

Acknowledgement

Support of this work by the Engineering and Physical Sciences Research Council (EPSRC) of the UK is gratefully acknowledged.

Appendix A. Supplementary data

Supplementary data associated with this article can be found, in the online version, at <http://dx.doi.org/10.1016/j.apcatb.2015.09.052>.

References

- [1] N.A.M. Razali, K.T. Lee, S. Bhatia, A.R. Mohamed, *Renew. Sustain. Energy Rev.* 16 (2012) 4951–4964.
- [2] M. Tahir, N.S. Amin, *Renew. Sustain. Energy Rev.* 25 (2013) 560–579.
- [3] N.S. Spinner, J.A. Vega, W.E. Mustain, *Catal. Sci. Technol.* 2 (2012) 19–28.
- [4] R.W. Dörner, D.R. Hardy, F.W. Williams, H.D. Willauer, *Energy Environ. Sci.* 3 (2010) 884–890.
- [5] S. Paulussen, B. Verheyde, X. Tu, C. De Bie, T. Martens, D. Petrovic, A. Bogaerts, B. Sels, *Plasma Sources Sci. Technol.* 19 (2010) 034015.
- [6] X. Tu, J.C. Whitehead, *Appl. Catal. B Environ.* 125 (2012) 439–448.
- [7] H.L. Chen, H.M. Lee, S.H. Chen, M.B. Chang, S.J. Yu, S.N. Li, *Environ. Sci. Technol.* 43 (2009) 2216–2227.
- [8] H.L. Chen, H.M. Lee, S.H. Chen, Y. Chao, M.B. Chang, *Appl. Catal. B Environ.* 85 (2008) 1–9.
- [9] E.C. Neyts, A. Bogaerts, *J. Phys. D Appl. Phys.* 47 (2014) 224010.
- [10] X. Tu, H.J. Gallon, M.V. Twigg, P.A. Gorry, J.C. Whitehead, *J. Phys. D Appl. Phys.* 44 (2011) 274007.
- [11] X. Tu, H.J. Gallon, J.C. Whitehead, *Catal. Today* 211 (2013) 120–125.
- [12] J. Van Durme, J. Dewulf, C. Leys, H. Van Langenhove, *Appl. Catal. B Environ.* 78 (2008) 324–333.
- [13] J.C. Whitehead, *Pure Appl. Chem.* 82 (2010) 1329–1336.
- [14] S.L. Brook, M. Marquez, S.L. Suib, Y. Hayashi, H. Matsumoto, *J. Catal.* 180 (1998) 225–233.
- [15] A. Indarto, J.-W. Choi, H. Lee, H.K. Song, *Environ. Eng. Sci.* 23 (2006) 1033–1043.
- [16] A. Indarto, D.R. Yang, J.W. Choi, H. Lee, H.K. Song, *J. Hazard. Mater.* 146 (2007) 309–315.
- [17] T. Mikoviny, M. Kocan, S. Matejcek, N.J. Mason, J.D. Skalny, *J. Phys. D Appl. Phys.* 37 (2004) 64–73.
- [18] M. Tsuji, T. Tanoue, K. Nakano, Y. Nishimura, *Chem. Lett.* (2001) 22–23.
- [19] J.Y. Wang, G.G. Xia, A.M. Huang, S.L. Suib, Y. Hayashi, H. Matsumoto, *J. Catal.* 185 (1999) 152–159.
- [20] S. Wang, Y. Zhang, X. Liu, X. Wang, *Plasma Chem. Plasma Process.* 32 (2012) 979–989.
- [21] Q.Q. Yu, M. Kong, T. Liu, J.H. Fei, X.M. Zheng, *Plasma Chem. Plasma Process.* 32 (2012) 153–163.
- [22] G.Y. Zheng, J.M. Jiang, Y.P. Wu, R.X. Zhang, H.Q. Hou, *Plasma Chem. Plasma Process.* 23 (2003) 59–68.
- [23] D. Mei, Y.-L. He, S. Liu, J.D. Yan, X. Tu, *Plasma Process. Polym.* (2015), <http://dx.doi.org/10.1002/ppap.201500159>.
- [24] R. Aerts, W. Somers, A. Bogaerts, *ChemSusChem* 8 (2015) 702–716.
- [25] M. Ramakers, I. Michiels, R. Aerts, V. Meynen, A. Bogaerts, *Plasma Process. Polym.* 12 (2015) 755–763.
- [26] A. Baylet, P. Marecot, D. Duprez, X. Jeandel, K. Lombaert, J.M. Tatibouet, *Appl. Catal. B Environ.* 113 (2012) 31–36.
- [27] H.B. Zhang, K. Li, T.H. Sun, J.P. Jia, Z.Y. Lou, L.L. Feng, *Chem. Eng. J.* 241 (2014) 92–102.

- [28] R. Snoeckx, R. Aerts, X. Tu, A. Bogaerts, *J. Phys. Chem. C* 117 (2013) 4957–4970.
- [29] X. Tu, H.J. Gallon, J.C. Whitehead, *J. Phys. D Appl. Phys.* 44 (2011) 482003.
- [30] X. Tu, B. Verheyde, S. Corthals, S. Paulussen, B.F. Sels, *Phys. Plasmas* 18 (2011) 080702.
- [31] L.F. Spencer, A.D. Gallimore, *Plasma Chem. Plasma Process.* 31 (2011) 79–89.
- [32] A. Fridman, *Plasma Chemistry*, Cambridge University Press, New York, 2008.
- [33] R. Aerts, T. Martens, A. Bogaerts, *J. Phys. Chem. C* 116 (2012) 23257–23273.
- [34] X.B. Zhu, X. Gao, C.H. Zheng, Z.H. Wang, M.J. Ni, X. Tu, *RSC Adv.* 4 (2014) 37796–37805.
- [35] F. Brehmer, S. Welzel, M.C.M. van de Sanden, R. Engeln, *J. Appl. Phys.* 116 (2014) 123303.
- [36] I.A. Semiokhin, Y.P. Andreev, *Russ. J. Phys. Chem.* 40 (1966) 1161.
- [37] H.H. Kim, A. Ogata, S. Futamura, *IEEE Trans. Plasma Sci.* 34 (2006) 984–995.
- [38] T. Hammer, T. Kappes, M. Baldauf, *Catal. Today* 89 (2004) 5–14.
- [39] H.J. Gallon, H.H. Kim, X. Tu, J.C. Whitehead, *IEEE Trans. Plasma Sci.* 39 (2011) 2176–2177.
- [40] X. Tu, H.J. Gallon, J.C. Whitehead, *IEEE Trans. Plasma Sci.* 39 (2011) 2172–2173.
- [41] W.S. Kang, J.M. Park, Y. Kim, S.H. Hong, *IEEE Trans. Plasma Sci.* 31 (2003) 504–510.
- [42] M. Zaka-ul-Islam, K. Van Laer, A. Bogaerts, 31th International Conference on Phenomena in Ionized Gases Granada, Spain, 2013.
- [43] H.L. Chen, H.M. Lee, S.H. Chen, M.B. Chang, *Ind. Eng. Chem. Res.* 47 (2008) 2122–2130.
- [44] O. Guaitella, L. Gatilova, A. Rousseau, *Appl. Phys. Lett.* 86 (2005) 151502.
- [45] L.G. Devi, G. Krishnamurthy, *J. Phys. Chem. A* 115 (2011) 460–469.
- [46] C. Subrahmanyam, M. Magureanu, D. Laub, A. Renken, L. Kiwi-Minsker, *J. Phys. Chem. C* 111 (2007) 4315–4318.
- [47] O. Guaitella, F. Thevenet, E. Puzeat, C. Guillard, A. Rousseau, *Appl. Catal. B Environ.* 80 (2008) 296–305.
- [48] A. Cybula, M. Klein, A. Zaleska, *Appl. Catal. B Environ.* 164 (2015) 433–442.
- [49] S. Xie, Y. Wang, Q. Zhang, W. Deng, Y. Wang, *ACS Catal.* 4 (2014) 3644–3653.
- [50] A.A. Assadi, A. Bouzaza, S. Merabet, D. Wolbert, *Chem. Eng. J.* 258 (2014) 119–127.
- [51] A.A. Assadi, J. Palau, A. Bouzaza, J. Penya-Roja, V. Martinez-Soriac, D. Wolbert, *J. Photochem. Photobiol. A* 282 (2014) 1–8.
- [52] T. Sano, N. Negishi, E. Sakai, S. Matsuzawa, *J. Mol. Catal. A Chem.* 245 (2006) 235–241.
- [53] A.E. Wallis, J.C. Whitehead, K. Zhang, *Catal. Lett.* 113 (2007) 29–33.
- [54] I. Nakamura, N. Negishi, S. Kutsuna, T. Ihara, S. Sugihara, E. Takeuchi, *J. Mol. Catal. A Chem.* 161 (2000) 205–212.
- [55] L.J. Liu, Y. Li, *Aerosol Air Qual. Res.* 14 (2014) 453–469.
- [56] X.Y. Pan, M.Q. Yang, X.Z. Fu, N. Zhang, Y.J. Xu, *Nanoscale* 5 (2013) 3601–3614.
- [57] N.A. Deskins, R. Rousseau, M. Dupuis, *J. Phys. Chem. C* 115 (2011) 7562–7572.
- [58] L.J. Liu, C.Y. Zhao, Y. Li, *J. Phys. Chem. C* 116 (2012) 7904–7912.
- [59] A. Mizuno, Y. Kisanuki, M. Noguchi, S. Katsura, S.H. Lee, U.K. Hong, S.Y. Shin, J.H. Kang, *IEEE Trans. Ind. Appl.* 35 (1999) 1284–1288.
- [60] W. Pipornpong, R. Wanbayor, V. Ruangpornvisuti, *Appl. Surf. Sci.* 257 (2011) 10322–10328.
- [61] L.B. Xiong, J.L. Li, B. Yang, Y. Yu, *J. Nanomater.* (2012) 831524.
- [62] A. Fujishima, T.N. Rao, D.A. Tryk, *J. Photochem. Photobiol. C Photochem. Rev.* 1 (2000) 1–21.
- [63] D.H. Mei, X.B. Zhu, Y.L. He, J.D. Yan, X. Tu, *Plasma Sources Sci. Technol.* 24 (2015) 015011.
- [64] H.J. Gallon, X. Tu, J.C. Whitehead, *Plasma Process. Polym.* 9 (2012) 90–97.
- [65] X.B. Zhu, X. Gao, R. Qin, Y.X. Zeng, R.Y. Qu, C.H. Zheng, X. Tu, *Appl. Catal. B Environ.* 170 (2015) 293–300.
- [66] A.E. Wallis, J.C. Whitehead, K. Zhang, *Appl. Catal. B Environ.* 74 (2007) 111–116.
- [67] A.E. Wallis, J.C. Whitehead, K. Zhang, *Appl. Catal. B Environ.* 72 (2007) 282–288.
- [68] T. Martens, A. Bogaerts, J. van Dijk, *Appl. Phys. Lett.* 96 (2010) 131503.